

Electronic Supplementary Information (ESI)

for

Metal Node Exchange-Driven Ligand-Strain Modulation Strategy for One-Dimensional Crystalline Coordination Polymers

Gengxin Wu,^a Yong-Kang Zhu,^a Dongxia Li,^a Jia-Rui Wu,^{a,b} Yan Wang,^{*a} Zhiquan Zhang,^{*a} and
Ying-Wei Yang^{*a}

^a College of Chemistry, Jilin University, 2699 Qianjin Street, Changchun 130012, P. R. China

^b Key Laboratory of Automobile Materials of Ministry of Education and School of Materials Science and Engineering, Jilin University, Changchun 130025, P. R. China

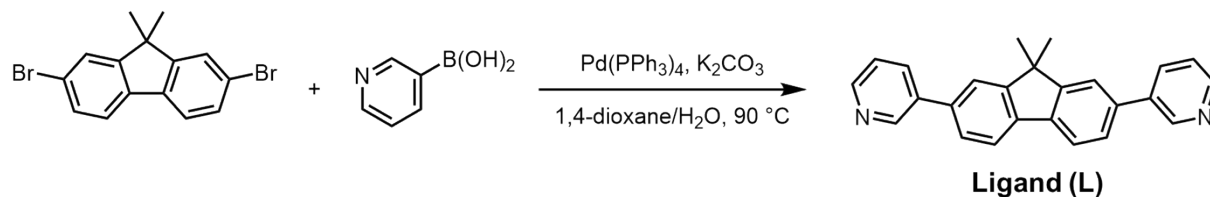
*E-mail: wangy2011@jlu.edu.cn; zzq@jlu.edu.cn; ywyang@jlu.edu.cn

1. Materials and methods

Unless otherwise noted, all reagents and solvents were commercially available and used without further purification. ^1H and ^{13}C NMR spectra were recorded at 298 K on a Bruker AVANCEIII 400 MHz instrument at room temperature. Chemical shifts were referred to TMS. Mass spectra were recorded on Bruker Daltonics Autoflex Speed Series: a Bruker Agilent1290-microTOF Q II High-resolution (HR) mass spectrometry instrument. Single-crystal X-ray diffraction data were recorded on a Bruker APEX-II CCD diffractometer using the ω -scan mode with graphite-monochromator Ga $K\alpha$ radiation ($\lambda = 1.34139$). Powder X-ray diffraction (PXRD) measurements were collected on a PANalytical B.V. Empyrean powder diffractometer operating at 40 kV/30 mA using the Cu $K\alpha$ line ($\lambda = 1.5418 \text{ \AA}$). Data were measured over the range of $5\text{-}50^\circ$ in $5^\circ/\text{min}$ steps over 8 min. UV-vis spectra were obtained on a Shimadzu UV-2550 spectrometer. The fluorescence spectra were recorded on a Shimadzu RF-5301PC fluorescence spectrophotometer. The time-resolved fluorescence decay curves and absolute fluorescence quantum yields were obtained on a FLS920 instrument (Edinburgh Instrument) with an excitation of 280 nm. Quantum yields were calculated using an integrating sphere. Thermogravimetric (TG) analysis was performed using a NETZSCH STA 449C instrument, and the samples were heated up to 900°C at a rate of $10^\circ\text{C min}^{-1}$ under a nitrogen atmosphere. The surface area analysis of samples was measured using a BET analyzer (Micrometrics ASAP 2020 PlusHD88) by nitrogen adsorption and desorption at 77 K. The sample was degassed at 120°C for 12 hours under a vacuum before the analysis. Scanning electron microscope (SEM) and energy dispersive spectroscopy (EDS) images were collected on a HITACHI SU8082 instrument. The X-ray photoelectron spectroscopy was carried out on a Shimadzu/Krayos AXIS Ultra DLD by sticking the powder sample to conductive paste.

2. Experimental section

2.1 Synthesis of ligand



Scheme S1. Synthesis of ligand (**L**).

2,7-Dibromo-9,9-dimethylfluorene (1.0 g, 2.8 mmol), 3-pyridylboronic acid (1.0 g, 8.4 mmol), Pd(PPh₃)₄ (0.3 g, 0.28 mmol) and K₂CO₃ (1.5 g, 11.2 mmol) were added in a mixed solvent of dioxane and water (5:1, 120 mL) in a flask. The resulting mixture was stirred under a nitrogen atmosphere at 90 °C for 12 hours. After evaporating the solvents, the residue was extracted with CH₂Cl₂ and then washed with water and brine. The organic layer was dried over anhydrous Na₂SO₄, concentrated under vacuum, and further purified by silica gel column chromatography to afford 0.9 g **L** (yield: 92%). ¹H NMR (400 MHz, CDCl₃, 298 K): δ 8.93 (d, *J* = 2.4 Hz, 2H), 8.62 (dd, *J* = 6.4, 2.0 Hz, 2H), 8.03 – 7.91 (m, 2H), 7.86 (d, *J* = 10.4 Hz, 2H), 7.66 (d, *J* = 1.6 Hz, 2H), 7.64 – 7.55 (m, 2H), 7.45 – 7.33 (m, 2H), 1.60 (s, 6H). ¹³C NMR (101 MHz, CDCl₃, 298 K): δ 154.8, 148.5, 148.4, 138.6, 137.3, 136.9, 134.4, 126.4, 123.6, 121.5, 120.9, 47.2, 27.3. HRMS (*m/z*): [M+H]⁺ calcd for C₂₅H₂₁N₂⁺, 349.1699, found 349.1614.

2.2 Preparation of Ag(I)-L and Cu(I)-L

AgNO₃ (19 mg, 0.1 mmol) or CuI (17 mg, 0.1 mmol) was dissolved in CH₃CN (6 mL) and added to CH₂Cl₂ (6 mL) solution of **L** (34.8 mg, 0.1 mmol). The mixture was stirred for 10 minutes to give a white (**Ag(I)-L**, 36 mg) or yellow (**Cu(I)-L**, 32 mg) precipitate. The precipitate was filtered off, washed several times with CH₃CN and CH₂Cl₂, and then dried under vacuum for further use.

2.3 Preparation of metal exchange products Ex-s and Ex-g

Ex-s: After the formation of **Ag(I)-L**, the dried powder (20 mg) was dispersed in CH₃CN. Subsequently, CuI (20 mg) was slowly added to the suspension under stirring, followed by another 5 min stirring at room temperature. Then, an obvious color change from white to yellow was observed. After removing the solvents, the resulting precipitate was washed with CH₃CN, H₂O, and a solution of KI, respectively, to afford the exchanged product **Ex-s**.

Ex-g: The mixture of **Ag(I)-L** (20 mg) and CuI (20 mg) was grounded in a mortar for 30 min, followed by washing with CH₃CN, H₂O, and the solution of KI, respectively, to afford the exchanged product **Ex-g**.

3. NMR and mass spectroscopy

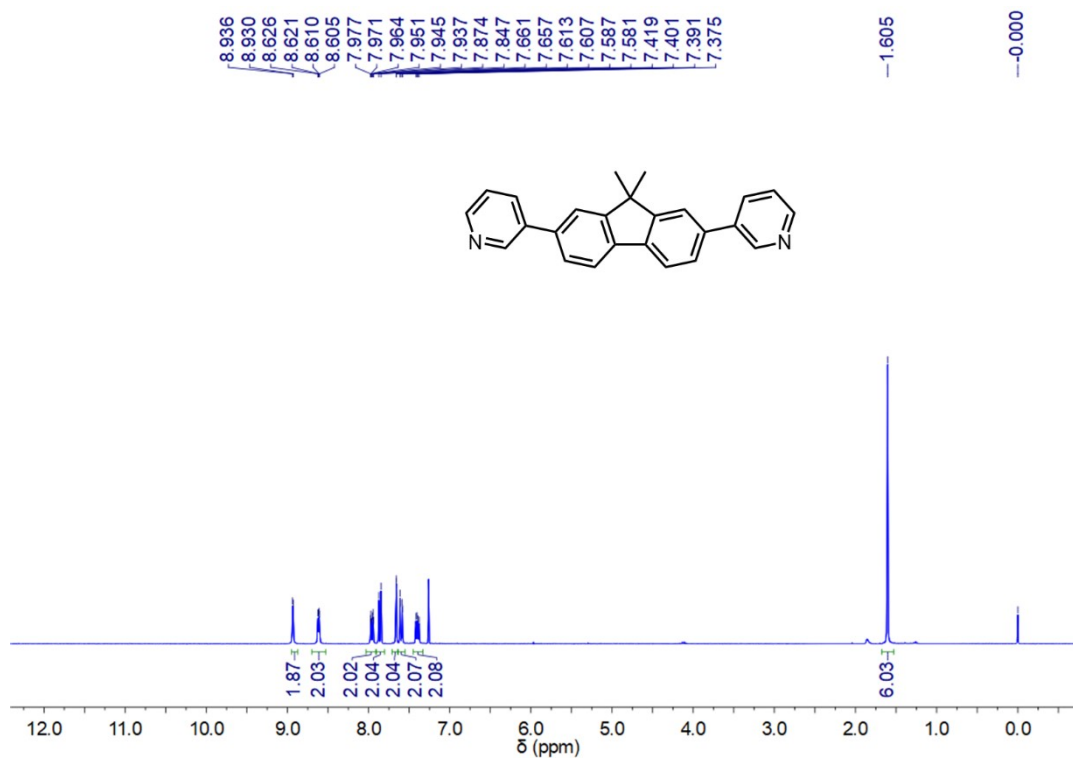


Figure S1. ¹H NMR spectrum (400 MHz, CDCl₃, 298 K) of **L**.

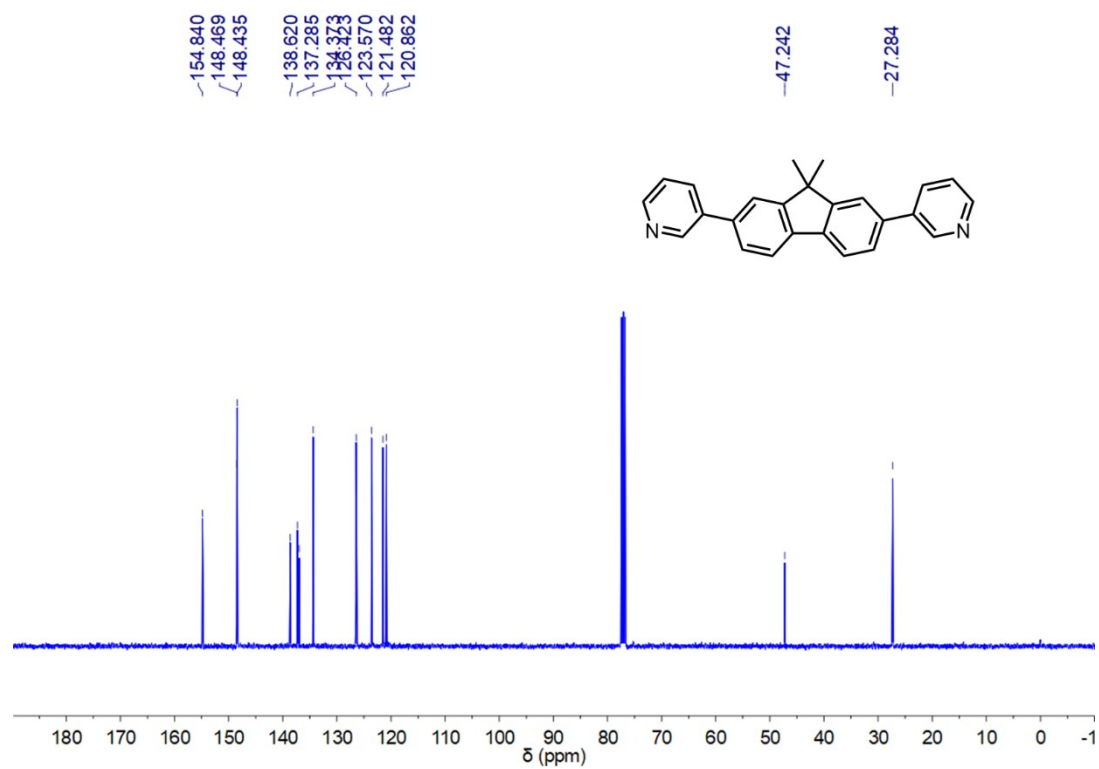


Figure S2. ¹³C NMR spectrum (101 MHz, CDCl₃, 298 K) of L.

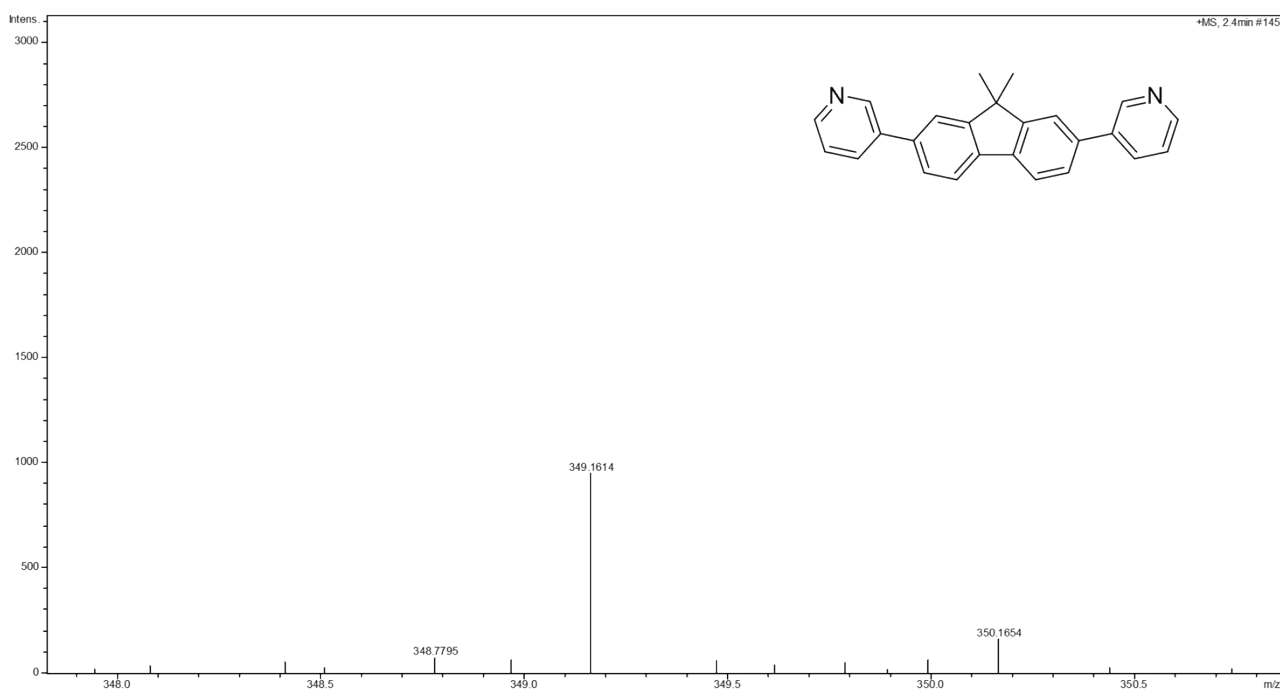


Figure S3. HRMS spectrum of L: [M+H]⁺ calcd for C₂₅H₂₁N₂⁺, 349.1699, found 349.1614.

4. Crystal structure analysis

Ag(I)-L: A solution of **Ag(I)-L** powder in dimethyl sulfoxide (0.5 mL) was added to a 2 mL glass bottle, followed by the addition of MeCN (0.2 mL), forming two distinct layers. Then colorless block crystals suitable for X-ray structural determination were obtained by slow diffusion of two phases after 24 hours.

Cu(I)-L: Yellow block crystals were grown by slow volatilization of a solution of **Cu(I)-L** powder in dimethyl sulfoxide (0.5 mL). After 24 hours, crystals suitable for X-ray structural determination were obtained.

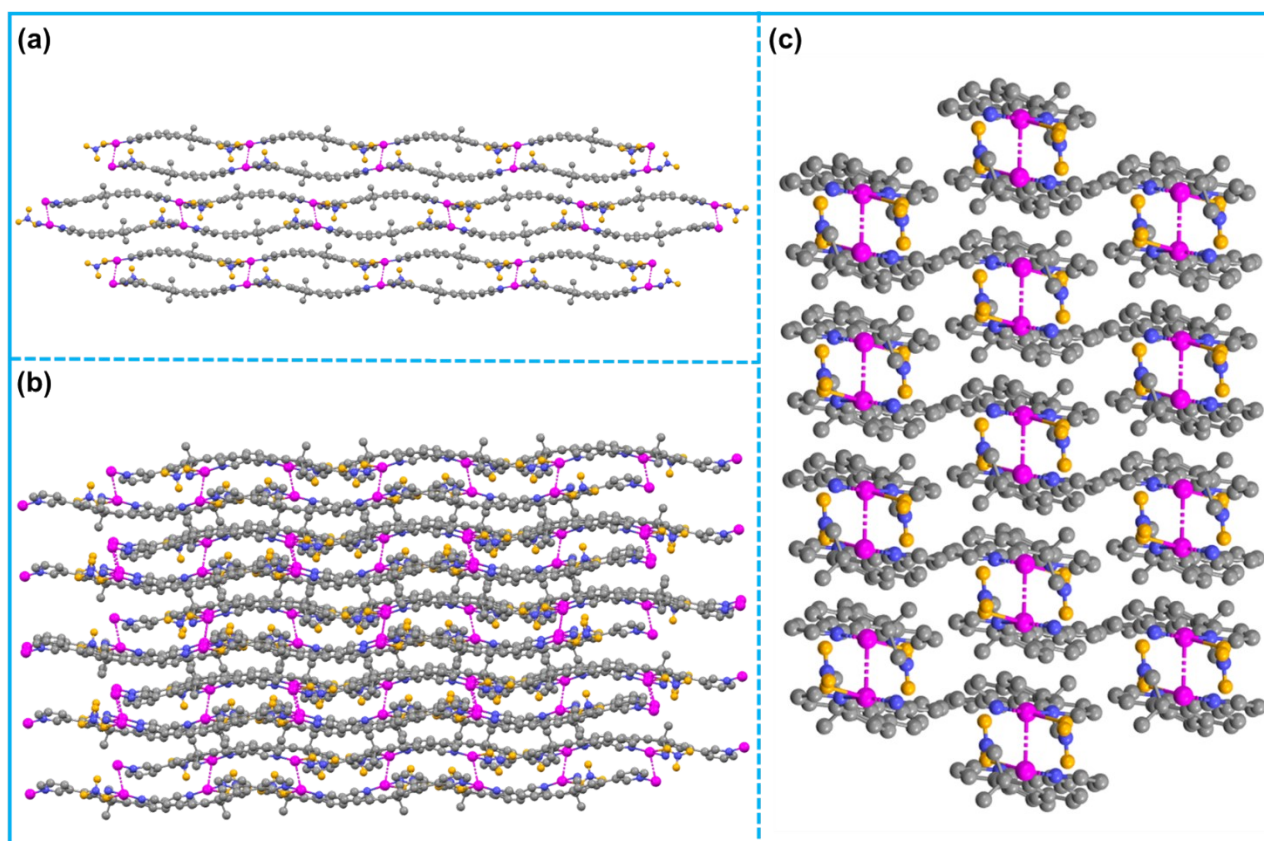


Figure S4. X-ray crystal structure and molecular packing of **Ag(I)-L** viewed along the *a*, *b*, and *c* axis. Hydrogen atoms are omitted for clarity.

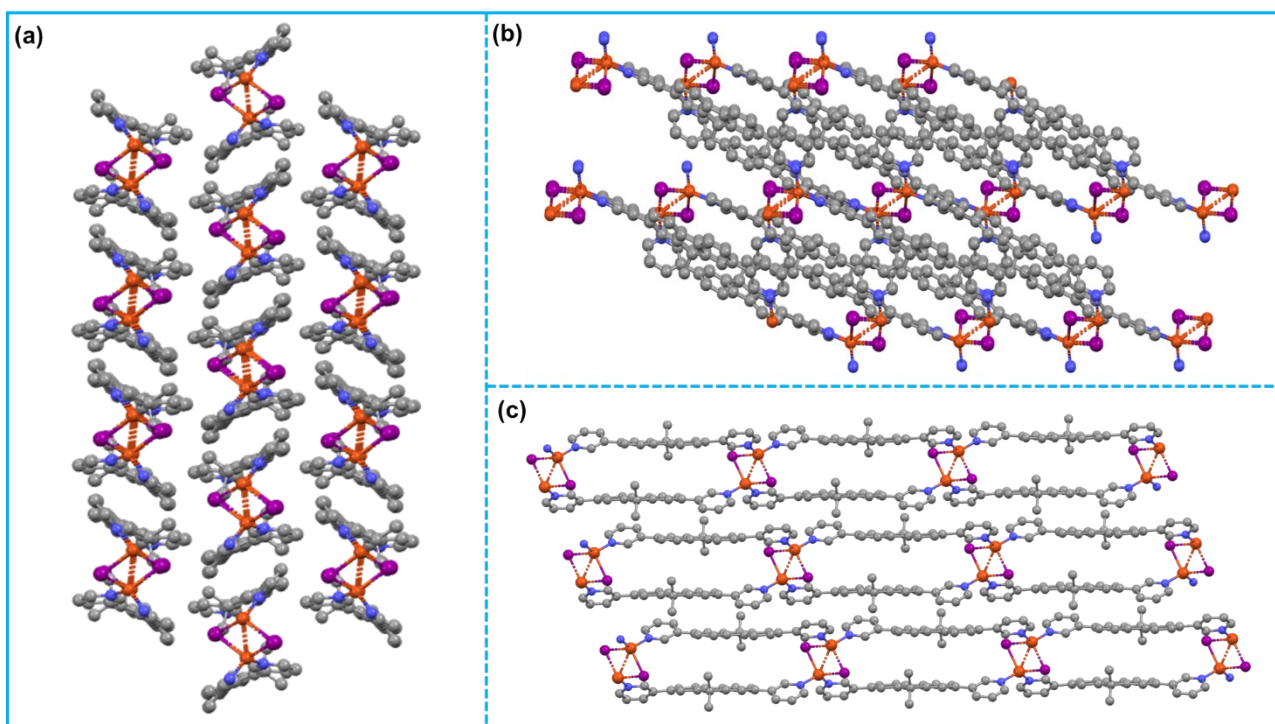


Figure S5. X-ray crystal structure and molecular packing of **Cu(I)-L** viewed along the *a*, *b*, and *c* axis. Hydrogen atoms are omitted for clarity.

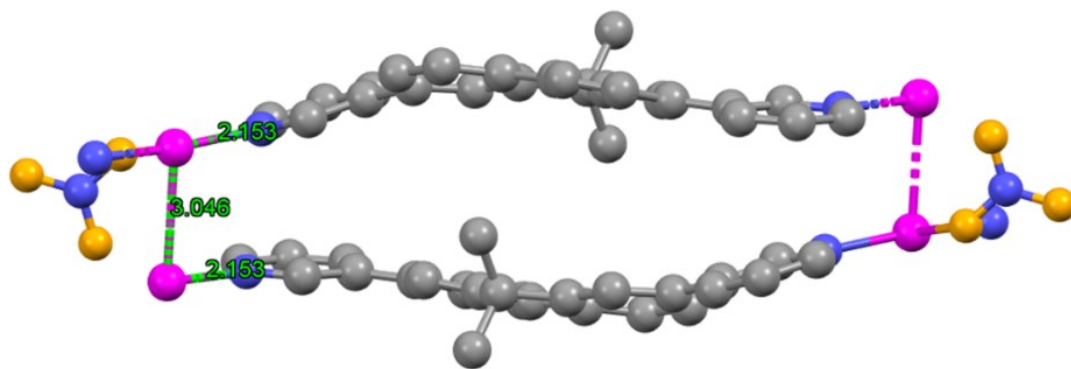


Figure S6. Illustration of the distance between Ag^+-Ag^+ connection and $\text{Ag}^+\cdots\text{N}$ bonds in **Ag(I)-L**.

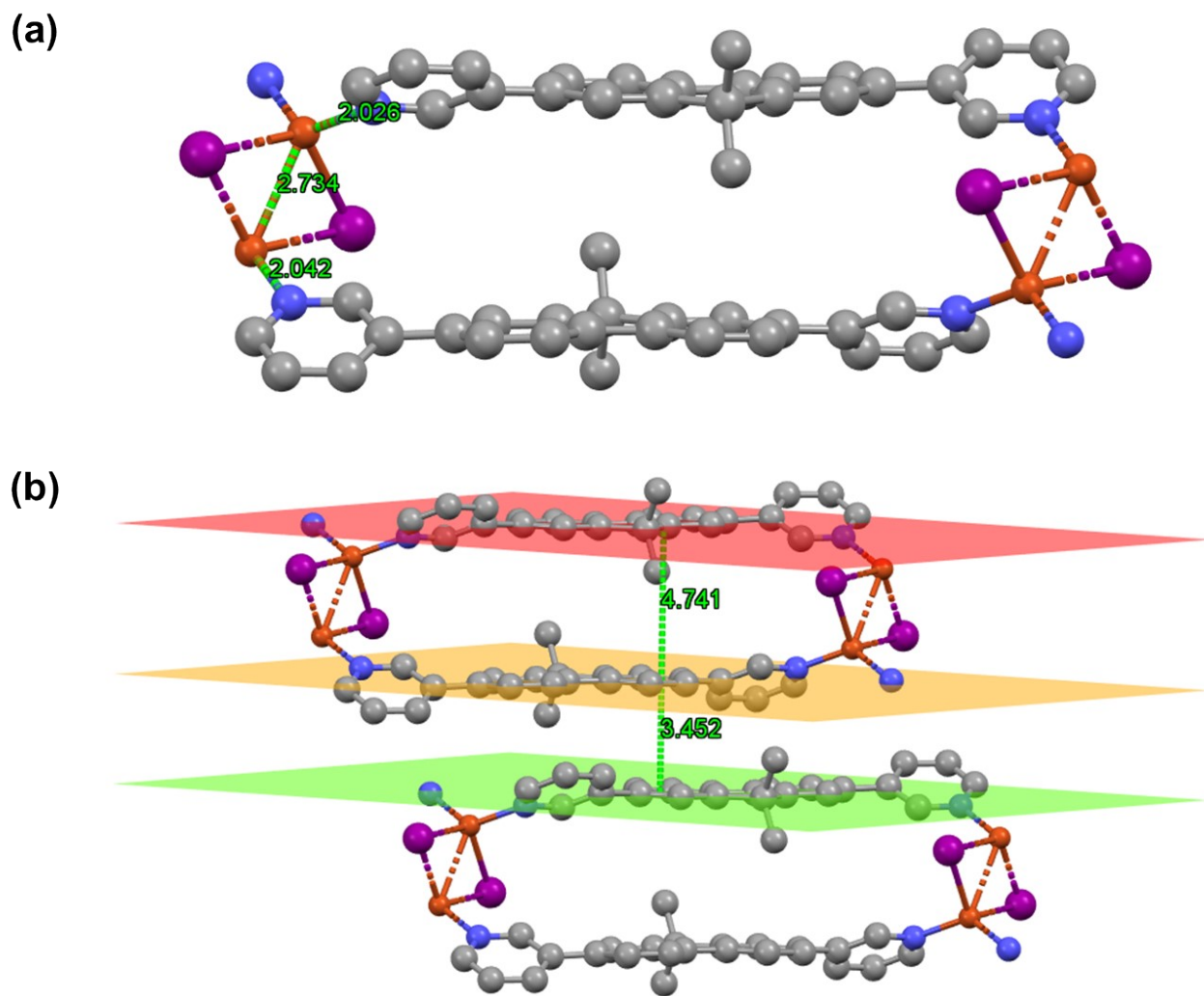


Figure S7. (a) Illustration of the distance between $\text{Cu}^+ - \text{Cu}^+$ connection and $\text{Cu} - \text{N}$ bonds. (b) The distances between the two parallel ligands and two adjacent ligands in $\text{Cu}(\text{I})\text{-L}$.

Table S1. Single crystal data of **Ag(I)-L** and **Cu(I)-L**

Compound	Ag(I)-L	Cu(I)-L
Empirical formula	C ₂₅ H ₂₀ AgN ₃ O ₃	C ₂₅ H ₂₀ CuIN ₂
Formula weight	517.86	538.88
Crystal system	monoclinic	monoclinic
Space group	P2 ₁ /n	P2 ₁ /c
<i>a</i> /Å	8.9941(7)	9.4863(7)
<i>b</i> /Å	16.8525(14)	14.7718(11)
<i>c</i> /Å	14.0933(12)	15.7131(12)
<i>a</i> /deg.	90	90
<i>b</i> /deg.	100.638(3)	101.323(3)
<i>γ</i> /deg.	90	90
<i>V</i> /Å ³	2099.5(3)	2159.0(3)
<i>Z</i>	42	43
ρ _{calc} /cm ³	1.640	1.658
μ/mm ⁻¹	5.332	13.054
<i>F</i> (000)	1048.0	1064.0
Theta range/deg.	7.188 to 114.602	7.212 to 114.178
Reflections collected	18789	20172
<i>R</i> (int)	0.0376	0.0441
R ₁ , wR ₂ [obs <i>I</i> > 2σ (<i>I</i>)]	R ₁ = 0.0246, wR ₂ = 0.0634	R ₁ = 0.0298, wR ₂ = 0.0746
R ₁ , wR ₂ (all data)	R ₁ = 0.0274, wR ₂ = 0.0649	R ₁ = 0.0341, wR ₂ = 0.0764
CCDC number	2333130	2333129

5. Characterizations of Ag(I)-L and Cu(I)-L

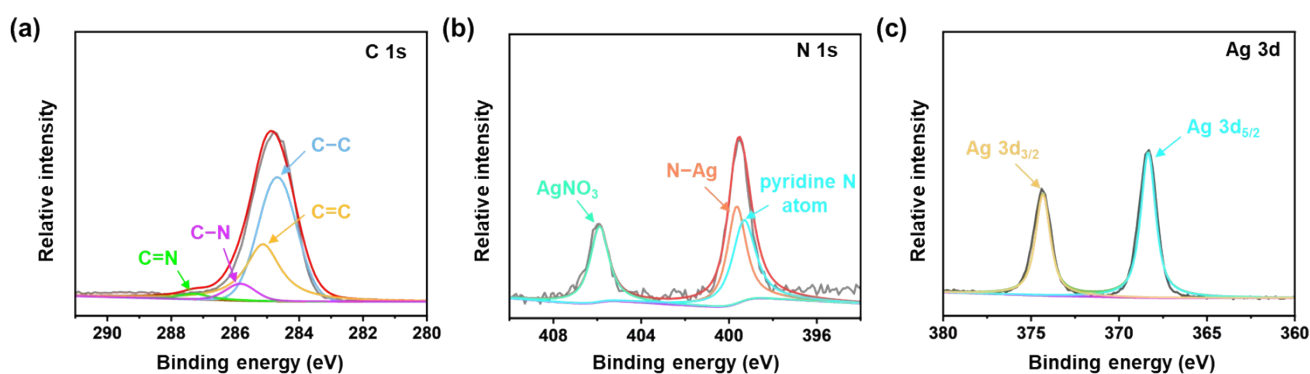


Figure S8. XPS spectra of Ag(I)-L. (a) C 1s, (b) N 1s, and (c) Ag 3d.

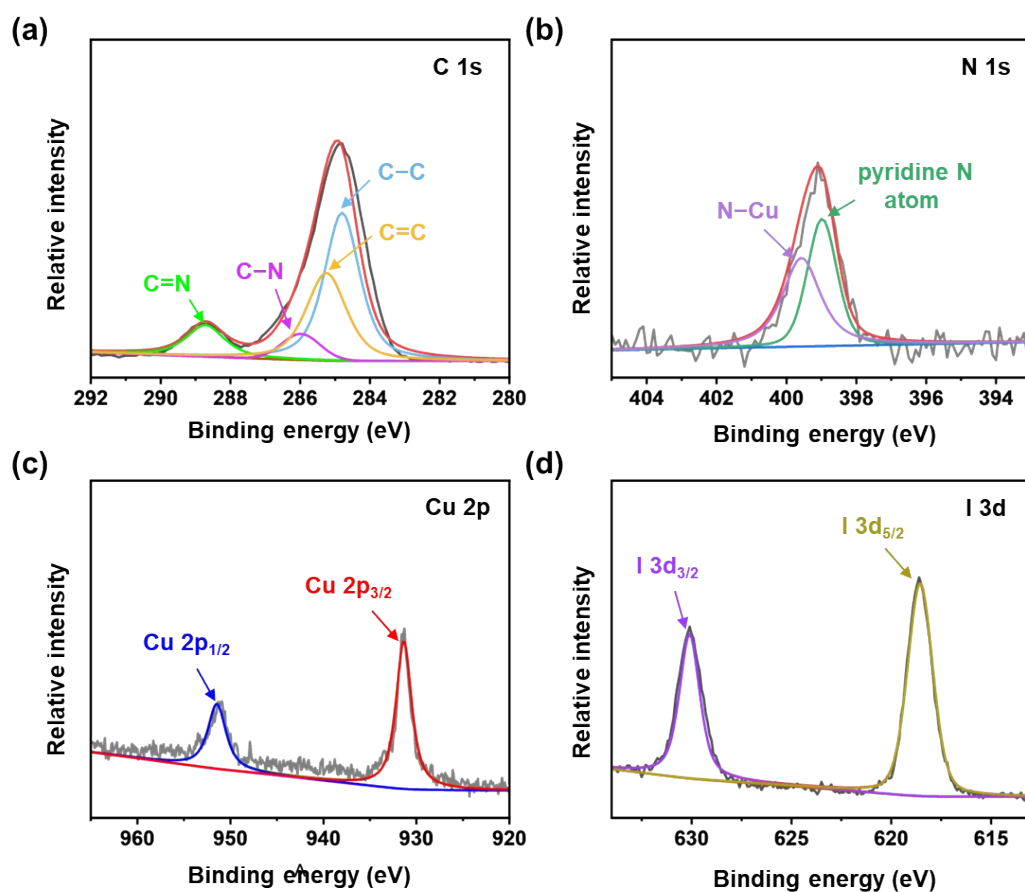


Figure S9. XPS spectra of Cu(I)-L. (a) C 1s, (b) N 1s, (c) Cu 2p, and (d) I 3d.

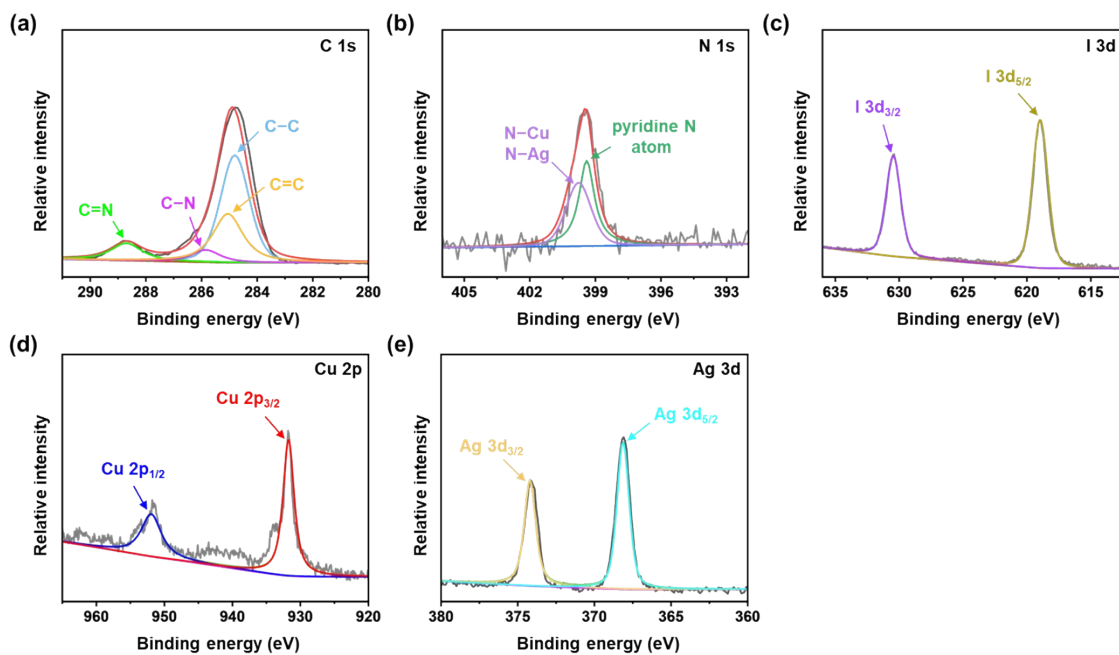


Figure S10. XPS spectra of *Ex-g*. (a) C 1s, (b) N 1s, (c) I 3d, (d) Cu 2p, and (e) Ag 3d.

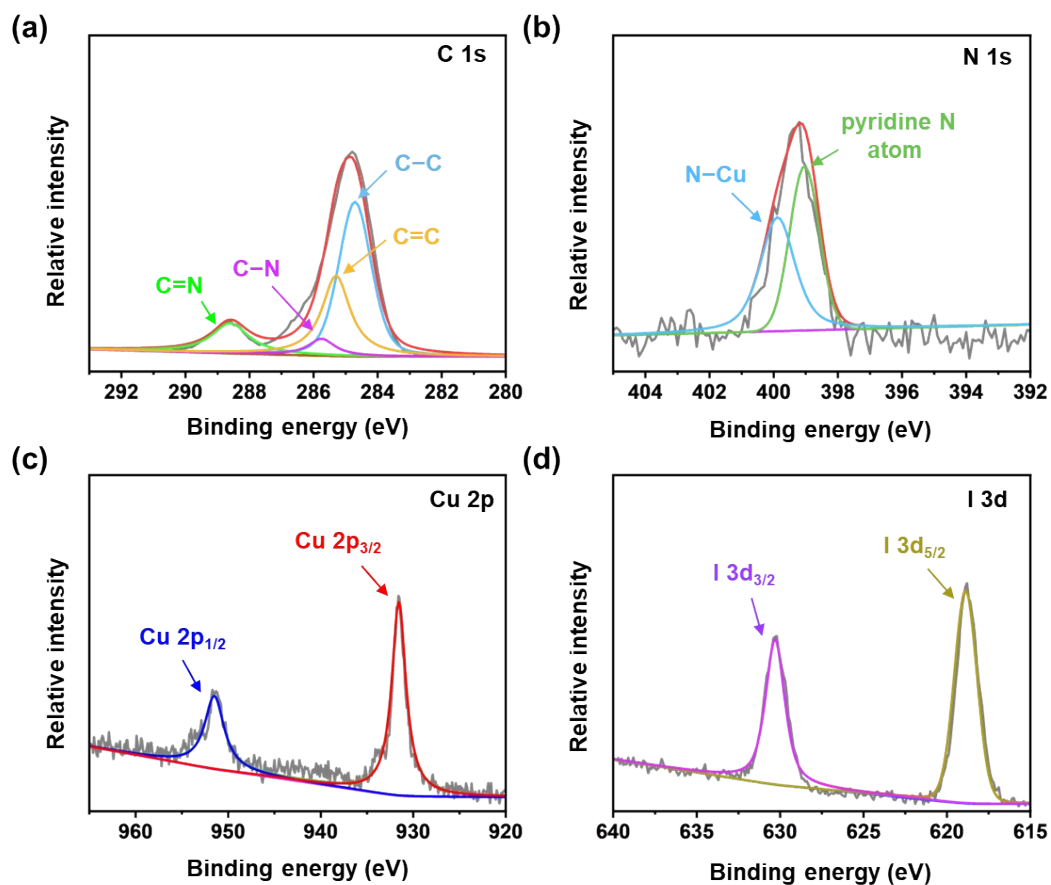


Figure S11. XPS spectra of *Ex-s*. (a) C 1s, (b) N 1s, (c) Cu 2p, and (d) I 3d.

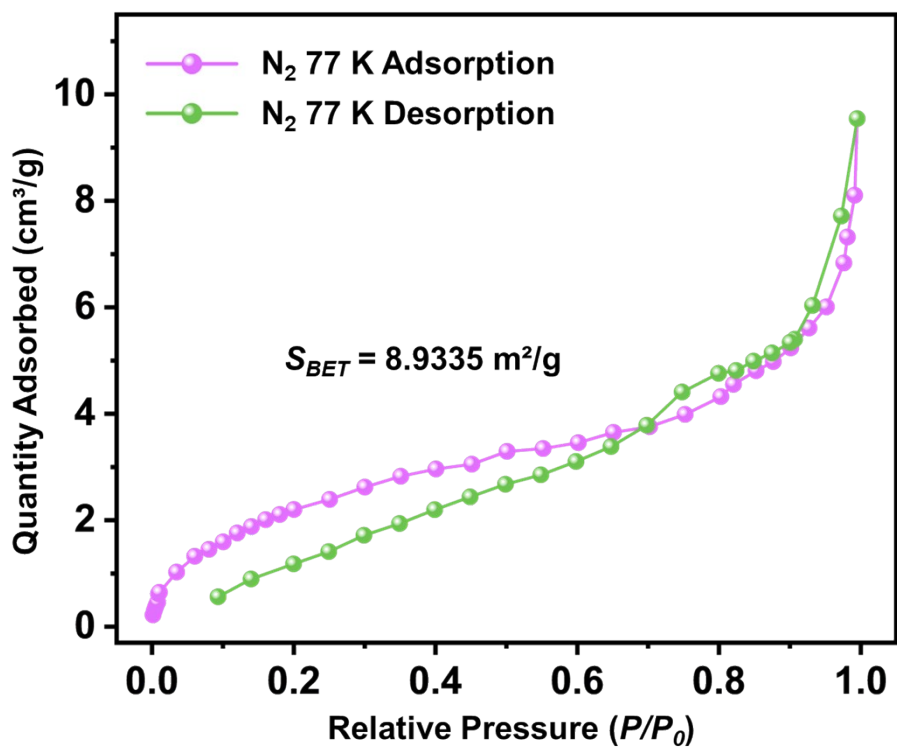


Figure S12. BET measurement of Ag(I)-L using N₂ at 77 K.

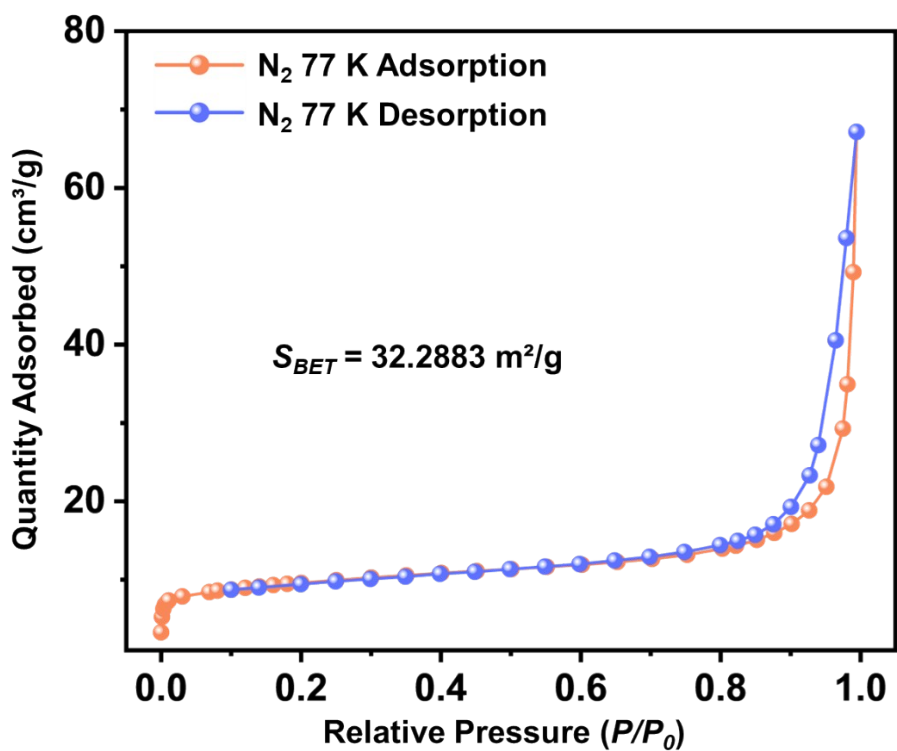


Figure S13. BET measurement of Cu(I)-L using N₂ at 77 K.

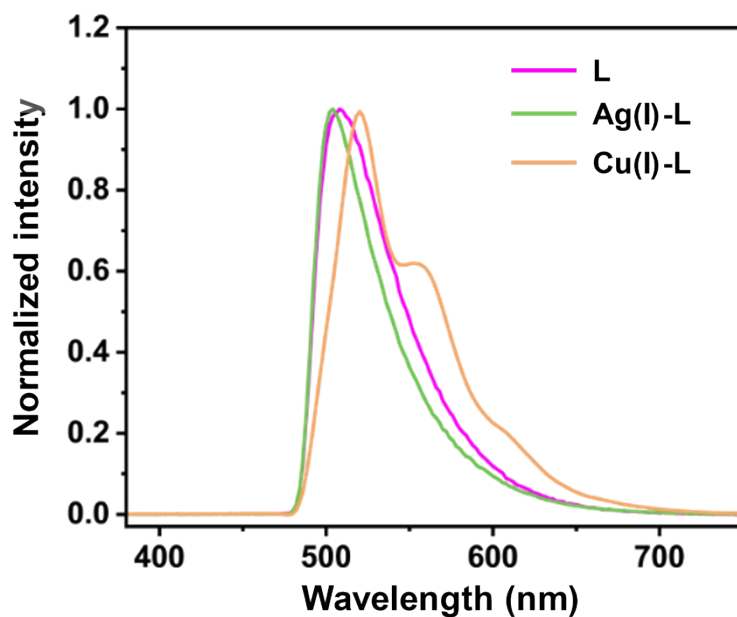


Figure S14. Normalized PL spectra of **L** (pink), **Ag(I)-L** (green), and **Cu(I)-L** (orange) in the solid states. Note: $\lambda_{ex} = 320$ nm.

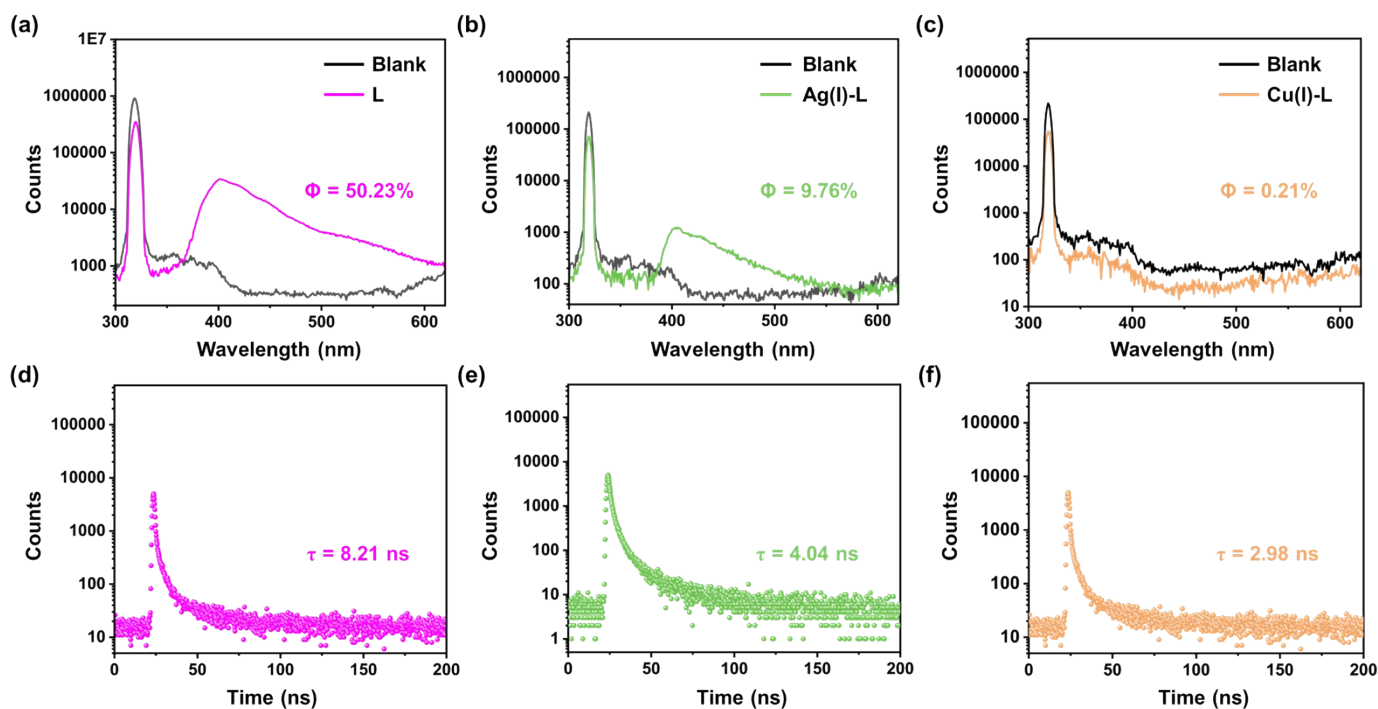


Figure S15. Fluorescence quantum efficiencies and lifetimes of (a,d) **L** (pink), (b,e) **Ag(I)-L** (green), and (c,f) **Cu(I)-L** (orange) in solid states. Note: $\lambda_{ex} = 320$ nm.

Table S2. Analytical results of Ag and Cu determined by ICP-AES

Sample	Method	Ag (%)	Cu (%)
Ag(I)-L	Calculated	20.81	0
	Experiment	9.83	0
Cu(I)-L	Calculated	0	11.79
	Experiment	0	16.91
Ex-s	Calculated	0	11.79
	Experiment	0.25	16.19
Ex-g	Calculated	0	11.79
	Experiment	6.58	13.64